The GLAST Tracker Design and Construction

R. Bellazzini[a] , L. Andreanelli[c], F. Angelini[a], S. Allegretti[g], R. Bagagli[a], L. Baldini[a], G. Barbiellini[d], F. Belli[c], A. Brez[a], M. Ceccanti[a], C. Cecchi[g], M. Ceschia[f], J. Cohen Tanugi[a], A. De Angelis[e], C. Favuzzi[b], F. Gargano[b], R. Giannitrapani[d], Giglietto[b], F. Giordano[b], M. Kuss[a], L. Latronico[a], F. Longo[d], F. Loparco[b], P. Lubrano[g], M.M. Massai[a], M.N. Mazziotta[b], M. Minuti[a], A. Morselli[c], N. Omodei[a], A. Paccagnella[f], C. Pagliarone[a], P. Picozza[c], M. Prest[d], S. Rainò[b], R. Rando[f], G. Spandre[a], P. Spinelli[b], L. Vigiani[a], F. Zetti[a]

[a]INFN-Pisa and University of Pisa, V. Livornese 1291, 56010 Pisa, Italy
[b]INFN-Bari, V. E. Orabona 4, 70126 Bari, Italy
[c]INFN-Roma2 and University of Roma "Tor Vergata", Via della Ricerca Scientifica 1, 00133 Roma, Italy
[d]INFN-Trieste and University of Trieste, V. Valerio 2, 34127 Trieste, Italy
[e]INFN-Trieste and University of Udine, Via delle Scienze 208, 33100 Udine, Italy
[f]INFN-Padova and University of Padova, V. Marzolo 8, 35131 Padova Italy
[g]INFN-Perugia, V. A. Pascoli, 06154, Perugia, Italy

The Gamma-ray Large Area Space Telescope (GLAST) is an international and multi-agency space mission that will study the cosmos in the energy range 20 MeV – 1 TeV. GLAST is an imaging gamma-ray telescope more much capable than instruments flown previously. The main instrument on board of the spacecraft is the Large Area Telescope (LAT), a high energy pair conversion telescope consisting of three major subsystems: a precision silicon tracker/converter, a CsI electromagnetic calorimeter and a segmented anti-coincidence system. In this article, we present the status of the construction and tests of the silicon tracker.

1. INTRODUCTION

EGRET[1], the Energetic Gamma Ray Experiment Telescope, launched in 1991 on board of the Compton Gamma Ray Observatory made the first complete survey of the sky above 30 MeV up to 10 GeV. It showed the high-energy gamma-ray sky to be surprisingly dynamic and observed a lot of gamma ray sources most of them still unidentified (no unambiguous counterparts at other wavelengths). The GLAST mission has been conceived to answer most of the important questions in high-energy astrophysics raised by results from EGRET. It will explore the uncovered energy spectrum from 20 MeV to 1 TeV.
GLAST [2] is a pair conversion telescope based on an $83m^2$ Silicon tracker and a high resolution, imaging CsI Electromagnetic calorimeter, all surrounded by an anticoincidence detector which is segmented to minimize self-veto from high energy electron backsplash from the calorimeter. The tracker/converter is a very complex device, with about 1 Million readout channels, instrumented with single side silicon strip detectors. A modular design and the large use of industrial partners allow a fast and high quality construction.

Respect to EGRET, GLAST will have a higher effective area (~ 6 times more), higher field of view, energy range and resolution, providing an unprecedented advance in sensitivity (a factor 30 or more).

GLAST is scheduled to be launched in September 2006 and it will be operational for a period of at least 5 years. It will reside in a low earth circular orbit (550 km altitude) at a 28.5-degree inclination.

This article presents the status of development and construction in Italy of the GLAST tracker.

2. THE LARGE AREA TELESCOPE (LAT)

High-energy gamma-rays are copiously produced at the sites of the most energetic accelerators in the Universe.

Above 10 MeV the primary interaction process of photons with matter is pair conversion: $\gamma \rightarrow e^+ + e^-$.

This process is the basis of the underlying measurement principle by providing a unique signature for gammas. The incident photon direction

is determined via the reconstruction of the trajectories of the resulting leptons pair (Fig. 1).
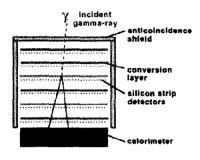

Figure1. Principle of a pair-conversion telescope.

The GLAST tracker consists of many layers of thin tungsten converter foils followed by silicon-strip tracking detectors. The electron and positron produced by the conversion are tracked with the silicon detectors and their energy measured by the calorimeter immediately below the tracker. The rejection of charged particles background (outnumbering the gamma rays flux by more than 5 orders of magnitude) will in large part rely on an outer, segmented, anticoincidence detector (ACD).
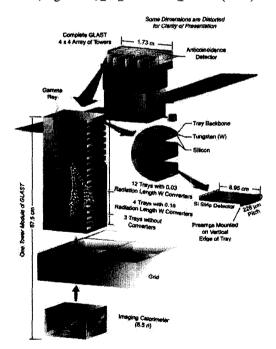

Figure 2. An exploded view of the LAT instrument.

The baseline GLAST instrument is structured in a modular design, consisting of a 4×4 array of identical towers (Fig. 2). Each 37×37-cm^2 *tower*

comprises a tracker, a calorimeter and a data acquisition module.

The LAT is self-triggered. Events that cause detector hits in three successive planes trigger the readout of each tower and of the anticoincidence system. Efficient rejection of charged particle background, >0.9997, is essential for GLAST to operate. The expected average raw trigger rate in orbit is a few kHz while the gamma-ray a few Hz.

3. TRACKER DESIGN OVERVIEW AND ASSEMBLY

Fig. 3 shows a view of a tracker tower module. It consists of a stack of 19 composite panels (*trays*) with 18 x,y detection planes, enclosed in Carbon fiber walls. The tray structure is a low mass carbon-composite assembly formed of a closeout, face sheets and vented Al honeycomb core. The tray structure holds the W converters, and is instrumented with silicon strip detectors (SSDs) on top and bottom and front-end electronics. There are:

• 12 trays with 3% R.L. W converter
• 4 with 18% R.L. W converter
• 3 with no converter foils.

Every tray is rotated by 90° from the preceding tray so each W foil is followed immediately by an x,y plane of detectors with a 2 mm gap between x and y oriented detectors.

The trays are stacked on top of each other and aligned to the sidewalls.

The bottom tray has a flange to mount on the grid. The tray structure has been designed to be sufficiently stiff to avoid tray-tray collision during launch.
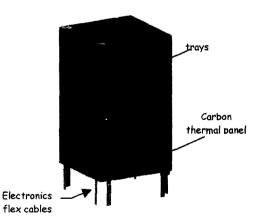

Figure 3. Cutaway view of a tracker tower module.

4. TRACKER SSDS SPECIFICATIONS AND TESTS

The tracker design is based on single-sided, AC-coupled silicon strip detectors with p-type implants upon n-intrinsic silicon. 40 MΩ polysilicon resistors are used to bias the implants. The baseline detector is obtained by wire bonding 4 8.95×8.95-cm^2 detectors (cut from 6-inch wafers) together into a 35.8-cm ladder. 4 ladders are glued on each face of each tray. The strip pitch is 228μm. There are 384 strips per ladder. The substrate thickness is 400μm and the resistivity > 5 kΩcm.

2200 detectors produced in this technology, out of 11500 eventually needed, have already been procured from Hamamatsu Photonics (HPK). Nearly 1900 have undergone electrical and dimensional tests with excellent results. To verify that the quality of the detectors conform to the contractual requirements, two types of electrical measurements are being performed in the Italian collaboration labs:

Figure 4a. Total leakage current vs. bias voltage.

- measurement of leakage current I as a function the bias voltage V (I-V curve, Fig. 4a).

- measurement of the body capacitance C as a function of the bias voltage V (C-V curve, Fig. 4b).
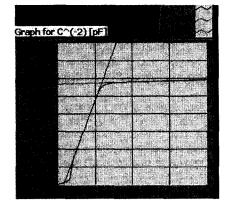

Figure 4b. Inverse squared of the body capacitance vs. bias voltage.

The sensor specifications for acceptance [3] require, to reduce the shot noise, an average leakage current at 150 V less than 200 nA and a maximum of 500 nA. Due to this low value of current the time consuming measurement of leakage current on every strip can be avoided and only the entire current on the detector is measured. A calibrated Keithley p-ammeter is used for this measurement.

With the C-V measurement both the body capacitance at 150 V and the depletion voltage V_D are evaluated. V_D is determined by applying the following definition:

$$(1/C^2_{(V)} - 1/C^2_{(V-\Delta V)} < 0.0039 \text{ nF}^{-2}) , V_D = V.$$

This measurement is performed using a calibrated HP LCR meter at 1kHz frequency.

The sensor specifications require low (<120 V) and quite uniform depletion voltage to reduce power consumption and noise.

In both measurements all strips are grounded, while the backplane is connected to variable (0÷200V) positive voltage.

A sample of 1375 sensors has been tested and the following average values have been obtained at 21°C and ~40% humidity:

- average leakage current = 99 nA
- average depletion voltage = 70 V
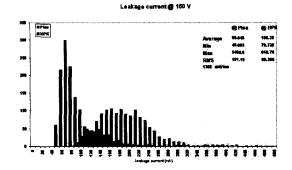- average body capacitance = 1837 pF.

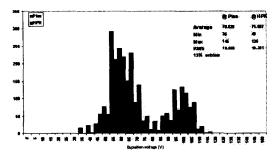Figure 5a. Leakage current distribution at 150 V.

Figure 5b. Depletion voltage distribution.

Figs. 5a,b,c, show the results of these measurements compared to the same tests made by Hamamatsu. Differences in leakage current between measurements

made in HPK and in Italy are due to differences in temperature and humidity.

V_D and bulk capacitance values agree quite well between different measurements and the narrow distribution of the body capacitance indicates good thickness uniformity between the substrates.

In a sample of 1903 sensors only 72 bad strips have been found, essentially all due to either shorted coupling capacitors or strip isolation, open along the strip in the implants and in the polysilicon resistors. This value corresponds to an extremely low fraction of bad strips, $\sim 10^{-5}$.

Figure 5c. Body capacitance distribution.

Geometrical measurements are also performed on the detector to control the saw cut quality and the mask alignment. The distances of the four reference cross centres, at each corner, to the X and Y edges is measured and the cut alignment derived by computing the shift, $(\Delta yA+\Delta yD)/2$, and rotation, $(\Delta yA-\Delta yD)$, parameters (see Fig. 6).
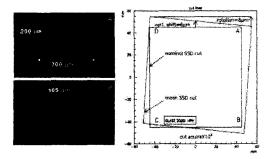

Figure 6. Cut alignment evaluation: shift and rotation measured in a wafer.

A maximum shift less than 1 μm and a rotation of 1.8 μm have been measured. In both cases shift and rotation values are well inside the specified range ± 10μm.

Up to now less than 2% of sensors have been rejected, most of them because of high current (>500 nA @120 V) and a few because of large change of IV curve slope below 150 V. Only a few detectors have been rejected for damages occurred in handling during lab tests or because chipped corners.

Only one was rejected for having depletion voltage > 120 V.

5. LADDER ASSEMBLY

To align and glue the four sensors to form a ladder a special jig has been fabricated (see Fig. 7). The first wafer is placed in the tool, a small spring pushes it in place against the reference edge and then vacuum is applied. The following wafer is then placed in the adjacent location after deposition of a controlled layer of glue on the cut edge and then pressed smoothly against the first one, and so forth.

Figure 7. Tool for alignment and gluing.

Ladder assembling and testing activities are performed in two qualified Italian factories: G&A Engineering (Oricola, AQ) and MIPOT (Cormons, GO). 140 ladder prototypes, from mechanical (not flight) wafers, have been produced up to now for an Engineering Model Tower.
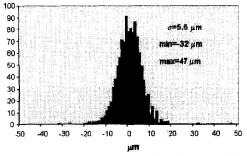

Figure 8. Wafers alignment errors in ladder assembly.

Geometrical measurements on these ladders have given alignment accuracy $\sigma = 5.5$ μm (Fig. 8). It is worth noting that this very good accuracy has been obtained without making use of any metrology with a coordinate measuring machine, but relying only on the precision of the cut line. After gluing, a special tool (Fig. 9a) is used to transfer the ladder to a service box for subsequent wire bonding and encapsulation (Fig. 9b).
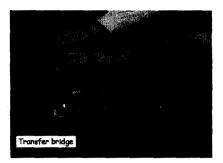
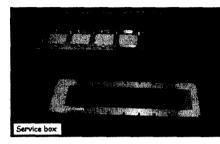Figure 9a. Transfer bridge.

Figure 9b. Service box for wire bonding.

Wire bonds are encapsulated for protection. Two different techniques have been tested: pure epoxy (3M Scotchweld 2216 A/B) and the so-called *dam* (3M Scotchweld 2216 A/B) and *fill* (General Electric 615) (Fig. 10). The latter has been chosen as more reliable.

Figure 10. Dam & fill encapsulation technique.

At each step, after bonding and after encapsulation the total leakage current of the ladder is measured. A maximum increase of the leakage current of 30% has been measured in one ladder at the end of the process (Fig. 11).

6. TRAY ASSEMBLY

Trays are of lightweight sandwich construction with a closeout frame. An exploded view of a tray is shown in Fig. 12.
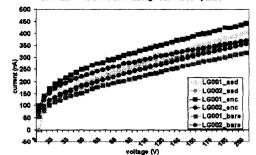

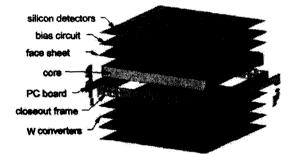Figure 11. Leakage current comparison after bonding and encapsulation.

Figure 12. Tray assembly sketch.

Plyform, a leading Italian factory in composite assembly, has been qualified for tray production.

Figure 13. Plyform SuperGLAST tray.

An example of tray with the thickest W converter foil (SuperGLAST tray) produced by Plyform is shown in Fig. 13.

Planarity within ±20 µm and an error in the overall dimensions of ±30 µm has been measured in the first prototype trays.

To assemble ladders on tray a special fixture has been fabricated. A sketch of the tool is shown in Fig. 14. A set of insertion pins (tray pins, bridge pins and guides, in figure) guarantees the alignment of the ladders on the tray.
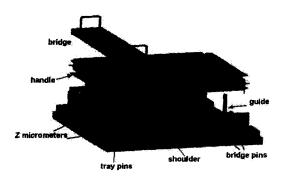
Figure 14. Ladder assembly fixture on tray.

Figs. 15a,b,c,d, show, in sequence, the procedure of ladders placement on a tray by means of the transfer bridge.
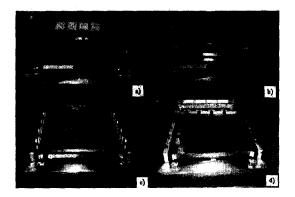

Figure 15. Ladder assembly procedure.

In Fig. 15a the Kapton bias circuit on top of the tray is visible. A space-qualified conductive adhesive is used to bond the backplane of the ladders to the bias circuit following the gluing pattern.

Preliminary vibration tests have been performed on SuperGLAST trays equipped with dummy wafers (Fig. 16). The first resonance frequency has been found at 626 Hz (Fig. 17a), well above the required fundamental frequency of 500 Hz, necessary to avoid tray-tray collisions during launch. Random-vibration tests independently on x,y,z and in a frequency range from 20Hz to 2kHz have also been performed.

Shaking in this way has not produced any detectable damage to the trays (Fig. 17b).

As tray qualification tests also include thermal tests, SuperGLAST trays have undergone four thermal cycles with temperature ranging from -30°C to +50°C in a climatic chamber. A thermal cycle lasts about 3 hours. Temperature is changed at a rate of 0.5 °C/min and is kept constant at the maximum and minimum value for about 2 hours (Fig. 18).
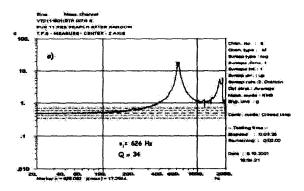

Figure 16. Vibration test set-up.

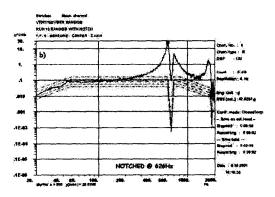Figure 17a. Normal mode search results.
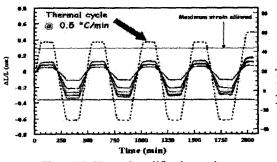

Figure 17b. Random vibration spectrum response

Figure 18. Thermal qualification cycles.

As shown in Fig. 18, the measured strain is much below the maximum strain allowed which is:

for $\Delta T = 25$ °C, $\Delta L/L \approx 100$ $\mu\varepsilon$,
for $\Delta T = -55$ °C $\Delta L/L < -350$ $\mu\varepsilon$.

Strain gauges have been applied in different positions on the top of the tray (Fig. 19).
FEA simulation of thermal cycling gives for $\Delta T = 25$°C a maximum expected stress, σ, of about 12 Mpa.
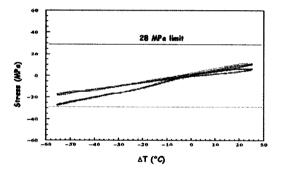

Figure 19. Thermal test set-up.

Figure 20. Thermal stress as a function of ΔT.

The measured thermal stress as a function of ΔT is shown in Fig. 20 for two different strain gauges. Maximum stress values resulting:

for $\Delta T = 25$ °C, $\sigma \approx 11$ Mpa,
for $\Delta T = -55$ °C, $\sigma \approx (-) 26$ Mpa,

well within the allowed limit of ± 28 Mpa drawn in the figure.

7. TOWER ASSEMBLY

A pre-Engineering model tower has been built using mock-up trays. For this purpose a tower assembly fixture has been designed and manufactured.

Fig. 21a shows the assembly jig with two trays already stacked one over the other, using the side-wall as external reference.
Assembly at SLAC of a full tower has gone very smoothly and has achieved good alignment (Fig. 21b). The tracker tower module will be subjected to a random-vibration test to full qualification levels at the NASA Ames Research Center.
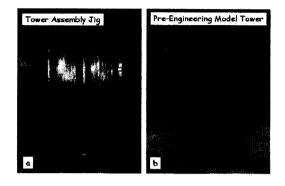

Figure 21. a) Tower assembly jig, b) full tower module.

8. CONCLUSIONS

The Italian GLAST collaboration is providing critical contribution to the LAT design and preparation for construction.
LAT prototyping activity has been successfully concluded. More than 1300 SSDs on a total of 2200 received from Hamamatsu have been already tested and selected for flight ladders assembly. Less than 2% of sensors have been rejected because not conform to the requirements of the key specifications.
Next actions are assembly and test of 300 flight ladders and construction of the Engineering model.

REFERENCES

[1] P. Nolan et al. IEEE Transactions Nucl. Sci.,39, 993-996.

[2] E. Bloom, G. Godfrey, S. Ritz, Proposal for the Gamma-ray Large Area Telescope, SLAC-R-22.February 1998.

[3] H. Sadrozinski, T. Ohsugi, GLAST LAT Procurement Specification, LAT-DS-00011-01.